JOURNAL OF CHEMICAL PHYSICS VOLUME 114, NUMBER 19 15 MAY 2001

# Transient resonance Raman spectroscopy and density functional theory investigation of iso-$CHBr_2Cl$ and iso-$CCl_3Br$ photoproducts produced following ultraviolet excitation of $CHBr_2Cl$ and $CCl_3Br$

Xuming Zheng,[a] Cheong Wan Lee, Yun-Liang Li, Wei-Hai Fang,[b]
and David Lee Phillips[c]
*Department of Chemistry, University of Hong Kong, Pokfulam Road, Hong Kong*

(Received 27 November 2000; accepted 5 March 2001)

We report transient resonance Raman spectra and density functional theory calculations for the photoproducts produced after ultraviolet excitation of $CHBr_2Cl$ and $CCl_3Br$ in cyclohexane solution. Comparison of the computed vibrational frequencies to the experimental Raman frequencies revealed that the iso-CHBrCl–Br and iso-CHClBr–Br species are mainly responsible for the transient resonance Raman spectrum observed following ultraviolet excitation of $CHBr_2Cl$. Similar comparisons for $CCl_3Br$ showed the iso-$CCl_2Cl$–Br species is mainly responsible for the transient resonance Raman spectrum observed following ultraviolet excitation of $CCl_3Br$. Additional density functional theory computations were done to examine the chemical reactions of iso-$CH_2Br$–Cl and iso-$CH_2Cl$–Br with ethylene to give cyclopropane and Br–Cl product. We briefly discuss the possibility for release of reactive halogens into the atmosphere via the photochemical and chemical reactions of iso-polyhalomethane molecules formed after ultraviolet excitation of polyhalomethanes in condensed phase environments.
[DOI: 10.1063/1.1367391]

## I. INTRODUCTION

Polyhalomethanes like $CHBr_3$, $CHBr_2Cl$, $CH_2IBr$, and $CH_2I_2$ have been observed in the atmosphere and are potentially important sources of reactive halogen species in the atmosphere.[1–8] Polyhalomethanes are also of interest in synthetic chemistry for cyclopropanation reactions.[9–13] Ultraviolet excitation of polyhalomethanes in the gas phase generally give rise to direct carbon–halogen (C–X) bond cleavage reaction(s).[14–26] For several polyhalomethane molecular systems, molecular beam anisotropy measurements indicate the direct photodissociation reactions take place in a time much less than a rotational period of the parent polyhalomethane molecule.[14,16–19] The polyatomic photofragments from these direct photodissociation reactions typically receive a large amount of internal excitation of their vibrational and rotational degrees of freedom as determined from translational photofragment spectroscopy experiments for $CH_2I_2$,[16] $CH_2BrI$,[19] and $CF_2I_2$.[20,21] This is consistent with the observation that the direct photodissociation reactions proceed along multidimensional reactions coordinates as deduced from resonance Raman investigations of the short-time photodissociation dynamics in both gas and solutions phases.[27–36]

Excitation of polyhalomethanes in the condensed phase results in more complex photodissociation dynamics and formation of interesting photoproduct species that are not observed in the gas phase.[37–46] For instance, ultraviolet photoexcitation, direct photoionization, and radiolysis of $CH_2I_2$ in condensed phase environments leads to formation of photoproduct(s) that have characteristic transient absorption bands ~385 nm (intense) and ~570 nm (moderate intensity) that have been ascribed to a number of species including trapped electrons,[37] the $CH_2I_2^+$ radical cation,[41,43] the $CH_2I$ radical,[44] and/or iso-$CH_2I$–I.[39,40,46] The solution phase photodissociation dynamics for $CH_2I_2$ has also been examined using femtosecond transient absorption spectroscopy experiments to examine the formation and decay of the photoproduct.[44–46] These studies showed similar features of a fast rise time followed by a fast decay and then a slow rise.[44–46] However, three different interpretations were given for the photodissociation processes depending on what photoproduct species was assumed to be responsible for the characteristic ~385 nm and ~570 nm transient absorption bands.[44–46] We recently used nanosecond[47] and picosecond[48] time-resolved resonance Raman experiments and density functional theory computations to directly probe the ~385 nm transient absorption band associated with the photoproduct produced after ultraviolet excitation of $CH_2I_2$ in room temperature solutions. Our studies[47,48] conclusively showed that the iso-$CH_2I$–I species is mainly responsible for the ~385 nm transient absorption band. Inspection of results from solution phase[44–48] and gas phase experiments[27–36] suggests that solvation is responsible for formation of iso-$CH_2I$–I product species via interaction of the initially formed $CH_2I$ and I photofragments with the solvent cage about the parent mol-

---

[a] Present address: Department of Applied Chemistry, Zhejiang Institute of Science and Technology, 88 Wenyi Road, Hangzhou 310033, People's Republic of China.

[b] Permanent address: Department of Chemistry, Beijing Normal University, Beijing 100875, People's Republic of China.

[c] Author to whom correspondence should be addressed. Electronic mail: phillips@hku.hk

ecule. We have also recently investigated a number of polyhalomethanes containing bromine and/or iodine atoms.[49–52] We found that isomers of these compounds are also formed after ultraviolet photoexcitation of the parent polyhalomethane in room temperature solutions[49–52] and this suggests that formation of iso-polyhalomethane species following ultraviolet excitation (usually $n\rightarrow\sigma^*$ transitions localized on C–X bonds) of polyhalomethanes in liquids is a common phenomena. So far we have focused our efforts on polyhalomethane molecules that contain bromine and iodine atoms.

In this paper we examine two polyhalomethanes that contain bromine and chlorine atoms ($CHBr_2Cl$ and $CCl_3Br$). We report transient resonance Raman spectra of the photoproducts produced after ultraviolet excitation of $CHBr_2Cl$ and $CCl_3Br$ in room temperature solutions and density functional theory calculations for species proposed to be products of the photodissociation reactions in the solution phase. We find that the iso-CHBrCl–Br and iso-CHClBr–Br species are formed following ultraviolet excitation of $CHBr_2Cl$ and the iso-$CCl_2Cl$–Br species is formed following ultraviolet excitation of $CCl_3Br$ in the solution phase. We have done additional density functional theory computations to examine the chemical reaction of iso-$CH_2Cl$–Br with ethylene to give cyclopropane and Br–Cl product. Since $CHBr_2Cl$ has been observed in noticeable concentrations in the troposphere,[7] we briefly discuss the possibility of simultaneous release of bromine and chlorine atoms via formation of Br–Cl from chemical reaction of the iso-CHBrCl–Br species with alkenes and/or terpenes in multiphase and/or heterogeneous media.

## II. EXPERIMENT AND CALCULATIONS

$CHBr_2Cl$ (98%) and $CCl_3Br$ (99%) and spectroscopic grade cyclohexane solvent (99.9+%) were used as received to make up samples of ~0.10–0.20 M for the transient resonance Raman experiments. Since the experimental apparatus and methods have been detailed elsewhere[47,49–53] only a short account will be given here. A Nd:YAG nanosecond pulsed laser harmonics and/or their hydrogen Raman shifted laser lines gave the pump and probe excitation wavelengths used for the Raman experiments. Spectra were obtained using a near collinear geometry to loosely focus and overlap the beams onto a flowing liquid stream of sample and pump–probe time-delays of ~0 ns and 10 ns were used. Spectra acquired at both time-delays appeared similar to one another. A backscattering geometry with reflective optics imaged the collected light through a depolarizer and entrance slit of a 0.5 m spectrograph which dispersed the light onto a liquid nitrogen cooled CCD. The Raman spectrum was accumulated for 300–600 s before being read out to an interfaced PC computer. Ten to twenty of these scans were added together to obtain spectra and the known frequencies of the cyclohexane vibrational bands were used to calibrate the Raman spectra. Subtraction of the pump-only and probe-only Raman spectra from the pump–probe Raman spectrum was done to extract the transient resonance Raman spectrum of the photoproduct and to remove solvent and parent Raman bands.

All of the density functional theory (DFT) computations reported here made use of the Gaussian program suite (G98W).[54] Complete geometry optimizations were done using C1 symmetry and B3LYP calculations.[54,55] Vibrational frequencies at the optimized geometry were computed for the species of interest. Time-dependent density functional theory at the random phase approximation[56] [TD(RPA)] was used to estimate the electronic absorption transition energies and oscillator strengths. The 6-311++G($d,p$) and/or aug-cc-PVTZ (Refs. 57, 58) basis sets were used for the DFT calculations.

The reactivity of the iso-polyhalomethanes containing chlorine and bromine atoms was explored using B3LYP calculations with $C_1$ symmetry for reactions of the iso-$CH_2Br$–Cl, iso-$CH_2Cl$–Br, $CH_2Br$, and $CH_2Cl$ species with ethylene. Since the dissociation of the isomer species involves formation of radicals, we used the complete active space SCF (CASSCF) approach[59–61] with an active space with ten electrons in eight orbitals [referred to as CAS(10,8) in the rest of the paper] to do the chemical reaction computations. The electrons in the active space originate mostly from the p electrons of the two halogen atoms. Analytical frequency computations were employed to determine whether the optimized structure was a minimum or a first-order saddle point and to find the zero-point energy correction. IRC computations were used to confirm the transition state connects the related reactants[62] and the standard 6-31+* basis set was used in the chemical reaction computations. Relativistic effects can influence the computed energy of a system that contains heavy atoms such as Br, but we are interested in the relative energies (barrier heights and reaction energies) in the chemical reaction calculations. The energy errors due to relativistic effects will partially cancel out in the computed relative energies and we expect that relativistic effects will have little influence on the reaction processes examined here. This is one of the reasons why polarization and diffuse functions were not used for the hydrogen atoms in the chemical reaction computations. The energies of the reactants and products were found by supermolecule computations where the intermolecular distance was fixed at 20 Å and these supermolecule calculations helped correct for the basis set superposition error.

## III. RESULTS AND DISCUSSION

### A. Transient resonance Raman spectra, density functional theory computational results, and assignment of iso-bromochloromethane species to the transient resonance Raman spectra

Figure 1 shows the ultraviolet absorption spectra of $CHBr_2Cl$ and $CCl_3Br$ in cyclohexane solution with the pump and probe excitation wavelengths used for the transient resonance Raman experiments shown above the spectra. Figure 2 shows transient resonance Raman spectra of the isomer photoproducts produced following ultraviolet photolysis of $CHBr_2Cl$ and $CCl_3Br$ in cyclohexane solution. These photoproduct spectra in Fig. 2 exhibit most of their resonance Raman intensity in the fundamentals, overtones and combination bands of several Franck–Condon active modes. The 282.4 nm excitation wavelength for the pump laser beam has

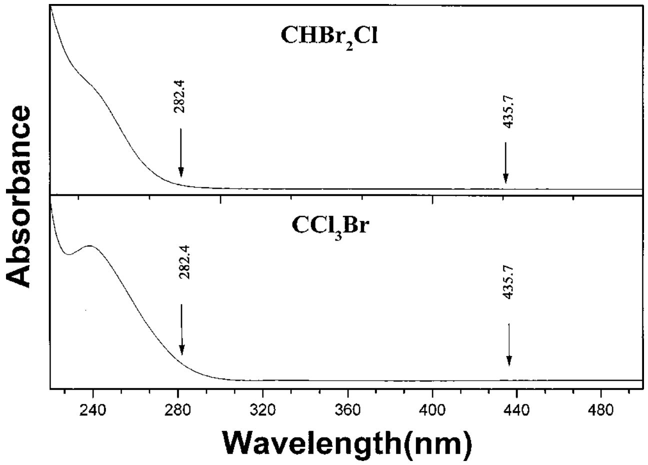

FIG. 1. Absorption spectra of $CHBr_2Cl$ (top) and $CCl_3Br$ (bottom) in cyclohexane solution with the pump (282.4 nm) and probe (435.7 nm) wavelengths used for the transient resonance Raman experiments indicated above the spectra.

enough photon energy to break noticeable amounts of the weaker C–Br bond but not the stronger C–Cl bond. Therefore, we generally considered the isomers and radical fragment species that would be formed by C–Br bond cleavage as well as the cation species of the parent polyhalomethane as possible candidates for the photoproduct(s) that may be responsible for the transient resonance Raman spectra observed in Fig. 2. The DFT computed optimized geometry parameters and vibrational frequencies for each of these possible photoproduct species are listed in Tables I and II, respectively.

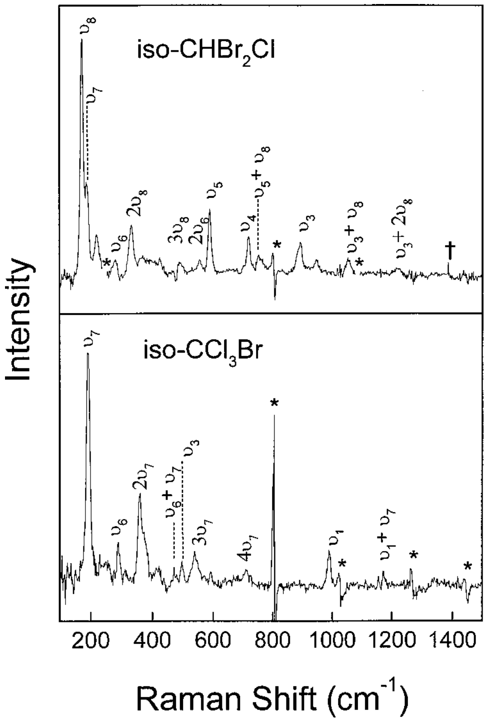

FIG. 2. Transient resonance Raman spectra of the isomer photoproducts produced from ultraviolet photolysis of $CHBr_2Cl$ (top) and $CCl_3Br$ (bottom) in cyclohexane solution obtained using 282.4 nm pump and 435.7 nm probe wavelengths. The assignments of some of the larger Raman bands are shown above the spectra (see text and Table II). The asterisks mark regions where solvent subtraction artifacts are present and the daggers label stray light or ambient light artifacts.

We compare the computed vibrational frequencies to those observed in the transient resonance Raman spectra of Fig. 2. The transient resonance Raman spectrum obtained following ultraviolet photolysis of $CHBr_2Cl$ in cyclohexane solution (shown at the top of Fig. 2) exhibits a number of Franck–Condon active vibrational modes. The strongest mode at 173 $cm^{-1}$ appears to have several overtones at $\sim 333\,cm^{-1}(\sim 2\times 173\,cm^{-1})$ and at $493\,cm^{-1}(\sim 3\times 173\,cm^{-1})$ as well as combination bands with other vibrational modes at 753 $cm^{-1}$ (about $589\,cm^{-1}+173\,cm^{-1}$), 1055 $cm^{-1}$ (about $894\,cm^{-1}+173\,cm^{-1}$) and 1216 $cm^{-1}$ (about $894\,cm^{-1}+2\times 173\,cm^{-1}$). The stronger fundamental resonance Raman bands at 173 $cm^{-1}$, 185 $cm^{-1}$, 589 $cm^{-1}$, 720 $cm^{-1}$, and 894 $cm^{-1}$ can be readily assigned to the iso-CHClBr–Br photoproduct species but not the iso-CHBrCl–Br, $CHBr_2Cl^+$ cation or CHClBr radical species. For example, the CHClBr radical species has no low frequency vibrational modes below 200 $cm^{-1}$ that are clearly present in the photoproduct Raman spectrum of Fig. 2 (i.e., the 173 $cm^{-1}$ and 185 $cm^{-1}$ fundamental bands). Therefore, the CHClBr radical can be ruled out as a species responsible for the transient resonance Raman spectrum. The $CHBr_2Cl^+$ cation has two computed vibrational modes in the 500–1000 $cm^{-1}$ region (at 561 $cm^{-1}$ and 808 $cm^{-1}$) while the photoproduct resonance Raman spectrum displays three fundamental modes in this region (at 589 $cm^{-1}$, 720 $cm^{-1}$, and 894 $cm^{-1}$). Therefore, we can also eliminate the $CHBr_2Cl^+$ cation as the species responsible for the transient resonance Raman spectrum shown at the top of Fig. 2. The photoproduct fundamental bands at 173 $cm^{-1}$, 185 $cm^{-1}$, 589 $cm^{-1}$, 720 $cm^{-1}$, and 894 $cm^{-1}$ exhibit good agreement with the fundamentals of the iso-CHClBr–Br species (i.e., the computed 166 $cm^{-1}$, 191 $cm^{-1}$, 618 $cm^{-1}$, 745 $cm^{-1}$, and 904 $cm^{-1}$ vibrational modes in Table II) but not the fundamentals of the iso-CHBrCl–Br species (i.e., the computed 181 $cm^{-1}$, 217 $cm^{-1}$, 635 $cm^{-1}$, 695 $cm^{-1}$, and 997 $cm^{-1}$ vibrational modes in Table II). Therefore, we assign the photoproduct fundamental bands at 173 $cm^{-1}$, 185 $cm^{-1}$, 589 $cm^{-1}$, 720 $cm^{-1}$, and 894 $cm^{-1}$ to the $\nu_8$, Br–Br stretch, $\nu_7$, C–Br–Br bend, $\nu_5$, C–H wag, $\nu_4$, Br–C–Cl sym. stretch, and $\nu_3$, Br–C–Cl asymmetric stretch vibrational modes of the iso-CHClBr–Br species.

The fundamentals, overtones, and combination bands of the iso-CHClBr–Br species account for most of the Raman intensity in the transient resonance Raman spectrum at the top of Fig. 2. However, there is still significant intensity in several other bands at 218 $cm^{-1}$, 281 $cm^{-1}$, 945 $cm^{-1}$ that appear to be due to a second photoproduct species. These Raman bands can be assigned to the iso-CHBrCl–Br species but not the $CHBr_2Cl^+$ cation or CHClBr radical species (see Table II). The C–Cl stretch vibrational frequency is computed to be at 997 $cm^{-1}$ for iso-CHBrCl–Br, at 808 $cm^{-1}$ for the $CHBr_2Cl^+$ cation and at 837 $cm^{-1}$ for the CHClBr radical. The experimental 945 $cm^{-1}$ Raman band agrees best with the iso-CHBrCl–Br species and we tentatively assign the 218 $cm^{-1}$, 281 $cm^{-1}$, 945 $cm^{-1}$ experimental Raman

TABLE I. Parameters for the optimized geometry computed from the B3LYP density functional theory computations for iso-polyhalomethane, polyhalomethane radical cation, and polyhalomethyl radical fragments proposed as photoproduct species formed following ultraviolet excitation of dibromochloromethane ($CHBr_2Cl$) and bromochloroform ($CCl_3Br$) in cyclohexane solution. Bond lengths are in Å and bond angles are in deg.

| Parameter | B3LYP Calc. | | | B3LYP Calc. | |
|---|---|---|---|---|---|
| For possible $CHBr_2Cl$ photoproducts | | | | | |
| Iso-CHClBr–Br | 6-311++G | aug-cc-PVTZ | iso-CHBrCl–Br | 6-311++G | aug-cc-PVTZ |
| *C*–Br$_1$ | 1.784 | 1.784 | C–Br$_1$ | 1.856 | 1.855 |
| Br$_1$–Br$_2$ | 2.699 | 2.700 | C–Br$_2$ | 2.632 | 2.492 |
| C–Cl | 1.691 | 1.699 | C–Cl | 1.6114 | 1.620 |
| C–H | 1.083 | 1.078 | C–H | 1.080 | 1.079 |
| C–Br$_1$–Br$_2$ | 127.2 | 127.2 | C–Cl–Br$_2$ | 124.8 | 124.4 |
| Br$_1$–C–Cl | 123.1 | 123.0 | Br$_1$–C–Cl | 122.9 | 122.9 |
| Br$_1$–C–H | 117.9 | 118.0 | Br$_1$–C–H | 115.8 | 115.9 |
| Cl–C–H | 115.5 | | Cl–C–H | 119.0 | 118.8 |
| D(Cl–C–Br$_1$–Br$_2$) | −80.3 | −80.4 | D(Br–C–Cl–Br) | −81.8 | −81.6 |
| D(H–C–Br$_1$–Br$_2$) | 77.5 | 77.1 | D(H–C–Cl–Br) | 80.5 | 80.1 |
| $CHBr_2Cl^+$ | | aug-cc-PVTZ | CHClBr radical | | aug-cc-PVTZ |
| C–Br | | 1.9846 | C–Br | | 1.870 |
| C–Cl | | 1.7024 | C–Cl | | 1.708 |
| C–H | | 1.0822 | C–H | | 1.078 |
| Br–C–Cl | | 116.5 | Cl–C–Br | | 120.0 |
| H–C–Cl | | 114.1 | Cl–C–H | | 117.0 |
| D(Br–C–Cl–Br) | | 105.5 | D(H–Br–C–Cl) | | 151.5 |
| D(H–C–Cl–Br) | | 127.3 | | | |
| For possible $CCl_3Br$ photoproducts | | | | | |
| iso-CCl$_2$Cl–Br | 6-311++G | aug-cc-PVTZ | | | |
| C–Cl$_1$ | 1.644 | 1.634 | | | |
| C–Cl$_2$ | 1.708 | 1.704 | | | |
| C–Cl$_1$–Br | 2.703 | 2.661 | | | |
| Cl$_1$–C–Cl$_2$ | 120.0 | 120.2 | | | |
| Cl$_2$–C–Cl$_2$ | 117.3 | 117.1 | | | |
| Br–Cl$_1$–C | 127.3 | 127.1 | | | |
| D(C–Cl–Cl–Cl) | −161.5 | −162.0 | | | |
| D(Br–Cl–C–Cl) | 80.3 | 80.7 | | | |
| $CBrCl_3^+$ cation | 6-311++G | | CCl$_3$ radical | | aug-cc-PVTZ |
| C–Cl$_1$ | 1.710 | | C–Cl | | 1.722 |
| C–Br | 2.103 | | Cl–C–Cl | | 116.9 |
| C–Cl$_3$ | 1.810 | | C–Cl–Cl–Cl | | 145.7 |
| Cl$_1$ or $_2$–C–Br | 111.3 | | | | |
| Cl$_3$–C–Br | 87.5 | | | | |

bands to the $\nu_7$Cl–Br stretch, $\nu_6$Br–C–Cl bend and $\nu_3$Br–C–Cl asymmetric stretch vibrational modes of the iso-CHBrCl–Br species. We note that the experimental 185 $cm^{-1}$ and 281 $cm^{-1}$ Raman bands could be reasonably assigned to both or either of the iso-CHClBr–Br and iso-CHBrCl–Br species since they have fundamentals that are nearly coincident with these two bands.

B3LYP time-dependent random phase approximation (TD/RPA) computations were done for each of the proposed photoproduct species in order to estimate their electronic transition energies and oscillator strengths and Table III lists the results of these calculations. We have previously used similar computations for $CH_2I_2$ and found reasonable agreement between experimental and computed values.[63] Inspection of Table III shows that both the iso-CHClBr–Br and iso-CHBrCl–Br species have very strong computed electronic transitions near 400 nm (at 397 nm with an oscillator strength of 0.4766 for iso-CHClBr–Br and at 406 nm with an oscillator strength of 0.4715 for iso-CHBrCl–Br). This is in reasonable agreement with the experimental transient absorption observed ~445 nm after ultraviolet excitation of $CHBr_2Cl$ in low temperature glasses.[37] However, no electronic transitions were computed for the 350 nm to 500 nm region for either the $CHBr_2Cl^+$ cation or CHClBr radical species in Table III. The DFT computations for the electronic transition energies and oscillator strengths provide further support for our assignment of the iso-CHClBr–Br and iso-CHBrCl–Br species as being the photoproducts responsible for the transient resonance Raman spectrum observed in Fig. 2 after ultraviolet excitation of $CHBr_2Cl$ in a room temperature solution of cyclohexane.

Our results for the ultraviolet photolysis of $CHBr_2Cl$ in room temperature solution indicates that solvent induced recombination of the initially produced CHClBr radical and Br fragment forms appreciable amounts of both the iso-CHClBr–Br and iso-CHBrCl–Br species. The different relative intensity for the resonance Raman bands for each of these photoproduct species in the transient resonance Raman

TABLE II. Comparison of experimental vibrational frequencies (in cm$^{-1}$) found from transient resonance Raman spectra to the B3LYP calculated vibrational frequencies for the species whose optimized geometry is given in Table I.

| Vibrational mode | B3LYP Calc. | | Transient resonance Raman vibrational frequency (in cm$^{-1}$) |
|---|---|---|---|
| iso-CHClBr–Br | 6-311++G | aug-cc-PVTZ | |
| $A'$ $\nu_1$, C–H stretch | 3207 | 3201 | |
| $\nu_2$, C–H scissor | 1259 | 1254 | |
| $\nu_3$, BrCCl asym. str. | 912 | 904 | 894 |
| $\nu_4$, Br–C–Cl sym. str. | 748 | 745 | 720 |
| $\nu_5$, C–H wag | 622 | 618 | 589 |
| $\nu_6$, Br–C–Cl bend | 275 | 273 | 281? |
| $\nu_7$, C–Br–Br bend | 191 | 191 | 185 |
| $\nu_8$, Br–Br str. | 165 | 166 | 173 |
| $\nu_9$, torsion | 55 | 55 | |
| iso-CHBr–Cl–Br | 6-311++G | aug-cc-PVTZ | |
| $A'$ $\nu_1$, C–H stretch | 3214 | 3208 | |
| $\nu_2$, C–H scissor | 1258 | 1254 | |
| $\nu_3$, BrCCl asym. str. | 1010 | 997 | 945 |
| $\nu_4$, Br–Cl sym. str. | 696 | 695 | |
| $\nu_5$, C–H wag | 643 | 635 | |
| $\nu_6$, Br–C–Cl bend | 285 | 283 | 281? |
| $\nu_7$, Cl–Br str. | 221 | 217 | 218 |
| $\nu_8$, C–Cl–Br bend | 184 | 181 | 185? |
| $\nu_9$, torsion | 53 | 51 | |
| CHBr$_2$Cl$^+$ cation | aug-cc-PVTZ | | |
| $A'$ $\nu_1$, C–H str. | 3177 | | |
| $\nu_2$, C–H bend | 1230 | | |
| $\nu_3$, C–H bend | 1080 | | |
| $\nu_4$, C–Cl str. | 808 | | |
| $\nu_5$, Br–C–Br sym. str. | 561 | | |
| $\nu_6$, Br–C–Br asym. str. | 484 | | |
| $\nu_7$, Cl–C–Br bend | 268 | | |
| $\nu_8$, Cl–C–H bend | 174 | | |
| $\nu_9$, Br–C–Br bend | 162 | | |
| CHClBr radical | aug-cc-PVTZ | | |
| $A'$ $\nu_1$, C–H str. | 3219 | | |
| $\nu_2$, C–H bend | 1206 | | |
| $\nu_3$, C–Cl str. | 837 | | |
| $\nu_4$, C–Br str. | 663 | | |
| $\nu_5$, C–H bend (o.p.) | 412 | | |
| $\nu_6$, Cl–C–Br bend | 242 | | |
| iso-CCl$_2$Cl–Br | 6-311++G | aug-cc-PVTZ | |
| $A'$ $\nu_1$, C–Cl stretch | 1012 | 1021 | 989 |
| $\nu_2$, ClCCl asym. str. | 910 | 907 | |
| $\nu_3$, CCl wag | 499 | 500 | 497 |
| $\nu_4$, Cl–C–Cl sym. str. | 388 | 388 | |
| $\nu_5$, Cl–C–Cl bend | 317 | 309 | |
| $\nu_6$, Cl–C–Cl bend | 297 | 288 | 289 |
| $\nu_7$, Cl–Br str. | 179 | 186 | 189 |
| $\nu_8$, torsion | 65 | 69 | |
| $\nu_9$, C–Cl–Br bend | 60 | 62 | |
| iso-CCl$_2$Br–Cl | 6-311++G | | |
| $A'$ $\nu_1$, C–Cl stretch | 871 | | |
| $\nu_2$, ClCCl asym. str. | 869 | | |
| $\nu_3$, CBr wag | 422 | | |
| $\nu_4$, Cl–C–Cl sym. str. | 407 | | |
| $\nu_5$, Cl–C–Cl bend | 253 | | |
| $\nu_6$, Cl–C–Br bend | 247 | | |
| $\nu_7$, Br–Cl str. | 212 | | |
| $\nu_8$, torsion. | 79 | | |
| $\nu_9$, C–Br–Cl bend | 48 | | |
| CBrCl$_3^+$ cation | 6-311++G | | |
| $A'$ $\nu_1$, Cl–C–Cl asym. str. | 880 | | |
| $\nu_2$, ClCCl asym. str. | 754 | | |
| $\nu_3$, Cl–C–Cl sym str. | 478 | | |
| $\nu_4$, C–Br str. | 400 | | |
| $\nu_5$, Cl–C–Br bend | 300 | | |
| $\nu_6$, Cl–C–Cl bend | 292 | | |
| $\nu_7$, Br–C–Cl bend | 168 | | |
| $\nu_8$, Cl–C–Cl bend | 116 | | |
| $\nu_9$, C–Br str. | 113 | | |
| CCl$_3$ radical | aug-cc-PVTZ | | |
| $A'$ $\nu_1$, C–Cl asym. str. | 860 | | |
| $\nu_2$, C–Cl asym. str. | 858 | | |
| $\nu_3$, C–Cl aym. str. | 479 | | |
| $\nu_4$, Cl–C–Cl bend (o.p.) | 329 | | |
| $\nu_5$, Cl–C–Cl bend | 269 | | |
| $\nu_6$, Cl–C–Cl bend | 268 | | |

at the top of Fig. 2 could be due to several factors such as different lifetimes, different relative resonance Raman en hancement and/or different yields for formation of the isomer photoproduct. We note that our recent study of the ultraviolet photolysis of CH$_2$BrI in room temperature solution found that only the iso-CH$_2$I–Br species could be observed on the nanosecond time scale following either *A*-band or *B*-band photoexcitation.[50] In contrast, only the iso-CH$_2$Br–I species was observed following *A*-band photoexcitation of CH$_2$BrI in low temperature solids (~12 K).[39,40] This suggested that although both iso-CH$_2$Br–I and iso-CH$_2$I–Br species may be initially produced following ultraviolet excitation of CH$_2$BrI in room temperature solution, only the more stable species had a sufficiently long lifetime to be observable in the nanosecond transient resonance Raman experiments.[50] Our current results for the ultraviolet photolysis of CHBr$_2$Cl indicate that the iso-CHClBr–Br and iso-CHBrCl–Br photoproduct species have similar stability in room temperature solutions.

The bottom of Fig. 2 shows the transient resonance Raman spectrum observed after ultraviolet excitation of CCl$_3$Br in room temperature cyclohexane solution. Inspection of this spectrum shows that the most intense band ~189 cm$^{-1}$ has several overtones (at ~368 cm$^{-1}$, ~538 cm$^{-1}$, and ~708 cm$^{-1}$) and a combination band at 1171 cm$^{-1}$ with the 989 cm$^{-1}$ fundamental. The transient resonance Raman spectrum for the CCl$_3$Br photoproduct species appears to have fundamental bands at 189 cm$^{-1}$, 289 cm$^{-1}$, 497 cm$^{-1}$, and 989 cm$^{-1}$. These fundamental bands can be readily assigned to the iso-CCl$_2$Cl–Br species but not to the iso-CCl$_2$Br–Cl molecule, CCl$_3$Br$^+$ cation or CCl$_3$ radical species. For example, the CCl$_3$ radical has no vibrational band below 200

TABLE III. Electronic absorption transition energies (singlet transitions) obtained from density functional theory calculations for the species whose optimized geometry is listed in Table I. The calculated oscillator strengths are given in parentheses. Only singlet transitions with wavelengths above 200 nm are listed.

| Molecule | URPA//UB3LYP/ | |
|---|---|---|
| For isomer species | | |
| iso-CHClBR–Br | 6-311++G | aug-cc-PVTZ |
| | **397 nm (0.5161)** | **397 nm (0.4766)** |
| | 396 nm (0.0195) | 395 nm (0.0579) |
| | 374 nm (0.0144) | 373 nm (0.0160) |
| | 239 nm (0.0006) | 240 nm (0.0005) |
| | 231 nm (0.0446) | 231 nm (0.0440) |
| | 202 nm (0.0426) | 201 nm (0.0283) |
| iso-CHBrCl–Br | 6-311++G | aug-cc-PVTZ |
| | 429 nm (0.0027) | 440 nm (0.0034) |
| | 416 nm (0.0931) | 428 nm (0.0904) |
| | **398 nm (0.4805)** | **406 nm (0.4715)** |
| | 229 nm (0.0017) | 231 nm (0.0013) |
| | 226 nm (0.0054) | 228 nm (0.0046) |
| | 211 nm (0.0127) | 214 nm (0.0120) |
| $CHBr_2Cl^+$ cation | | aug-cc-PVTZ |
| | | 1556 nm (0.1065) |
| | | 833 nm (0.0002) |
| | | 562 nm (0.0008) |
| CHClBr | | aug-cc-PVTZ |
| | | 273 nm (0.0012) |
| | | 209 nm (0.0001) |
| | | 204 nm (0.0010) |
| iso-$CCl_2Cl$–Br | 6-311++G | aug-cc-PVTZ |
| | 514 nm (0.0000) | 443 nm (0.0001) |
| | 502 nm (0.0022) | 432 nm (0.0605) |
| | **426 nm (0.6314)** | **419 nm (0.4986)** |
| | 227 nm (0.0788) | 225 nm (0.0469) |
| | 219 nm (0.0003) | 217 nm (0.0004) |
| iso-$CCl_2Br$–Cl | 6-311++G | |
| | 411 nm (0.3704) | |
| | 363 nm (0.0001) | |
| | 341 nm (0.0188) | |
| | 242 nm (0.0000) | |
| | 224 nm (0.2446) | |
| | 203 nm (0.1494) | |
| $CCl_3Br^+$ cation | 6-311++G | |
| | 1510 nm (0.0000) | |
| | 623 nm (0.0125) | |
| | 317 nm (0.0002) | |
| | 286 nm (0.0325); 284 nm (0.0001) | |
| | 241 nm (0.0000) | |
| | 222 nm (0.0000) | |
| | 214 nm (0.0009) | |
| | 211 nm (0.0030); 210 nm (0.0003) | |
| $CCl_3$ radical | | aug-cc-PVTZ |
| | | 256 nm (0.0000) |
| | | 200 nm (0.0049) |

$cm^{-1}$ or above 900 $cm^{-1}$ that can be attributed to the 189 $cm^{-1}$ or 989 $cm^{-1}$ photoproduct Raman bands. Thus, the $CCl_3$ radical can be ruled out as the photoproduct species responsible for the transient resonance Raman spectrum. Similarly, the iso-$CCl_2Br$–Cl species has no computed vibrational bands in the 100–200 $cm^{-1}$ region or above 900 $cm^{-1}$ and can also be ruled out as the species responsible for the transient resonance Raman spectrum. The $CCl_3Br^+$ cation has no computed vibrational modes above 900 $cm^{-1}$ and is also not likely associated with the transient resonance Raman spectrum for the $CCl_3Br$ photoproduct species. Inspection of the computed electronic transition energies and oscillator strengths for the possible photoproduct species (iso-$CCl_2Cl$–Br, $CCl_3Br^+$ or $CCl_3$) in Table III provides additional support for the assignment of the transient resonance Raman spectrum for the $CCl_3Br$ photoproduct to the iso-$CCl_2Cl$–Br species. The $CCl_3$ radical has no computed electronic transition above 300 nm and the $CCl_3Br^+$ cation has no computed electronic transition in the 400–500 nm region where the photoproduct species has a strong transient absorption responsible for the 435.7 nm transient resonance Raman spectrum (see bottom of Fig. 2). However, the iso-$CCl_2Cl$–Br species has a very strong electronic transition ~419 nm with an oscillator strength of 0.4986 that is consistent with its assignment as the photoproduct responsible for the 435.7 nm transient resonance Raman spectrum observed after ultraviolet excitation of $CCl_3Br$ in the solution phase. Thus, we assign the iso-$CCl_2Cl$–Br photoproduct experimental fundamental Raman bands as follows: 189 $cm^{-1}$ to the $\nu_7$ (Cl–Br stretch mode), 289 $cm^{-1}$ to the $\nu_6$ (Cl–C–Cl bend mode), 497 $cm^{-1}$ to the $\nu_3$ (C–Cl wag mode), and 989 $cm^{-1}$ to the $\nu_1$ (C–Cl stretch mode).

### B. Cyclopropanation reactions of olefins via ultraviolet photoexcitation of polyhalomethanes containing bromine and chlorine

We have previously noted[52] that there is experimental evidence in the literature[64] that iso-polyhalomethanes react with olefins to give a cyclopropanated product and a halogen molecule product. Ultraviolet excitation of polyhalomethanes in a 77 K matrix was found by Brown and Simon[64] to form ''color centers'' with characteristic intense transient absorption bands in the 350–470 nm region. When small amounts of olefins were added and the 77 K matrix permitted to warm up, new transient absorption bands ~310–320 nm were formed and shown to be due to a halogen molecule-olefin species (such as $I_2$-olefin and $Br_2$-olefin complexes).[64] The new transient absorption bands appeared with clean isobestic points from the ''color centers'' transient absorption bands (see Figs. 4 and 5 in Ref. 64). We have demonstrated that these ''color center'' intense transient absorption bands in the 350–470 nm region are really due to the iso-polyhalomethane species for a number of polyhalomethanes.[47–52] This and the results of previously reported experiments by Brown and Simons[64] suggests that iso-polyhalomethanes may react with olefins to produce a halogen molecule product that will then produce a halogen molecule-olefin complex. The following reaction scheme (where X=Cl, Br, I) is consistent with these observations:

Initiation Step
$$CH_2X_2 + h\nu \rightarrow CH_2X + X, \tag{1}$$

Recombination to produce isomer

$$CH_2X + X \rightarrow \text{iso-}CH_2X\text{–}X, \tag{2}$$

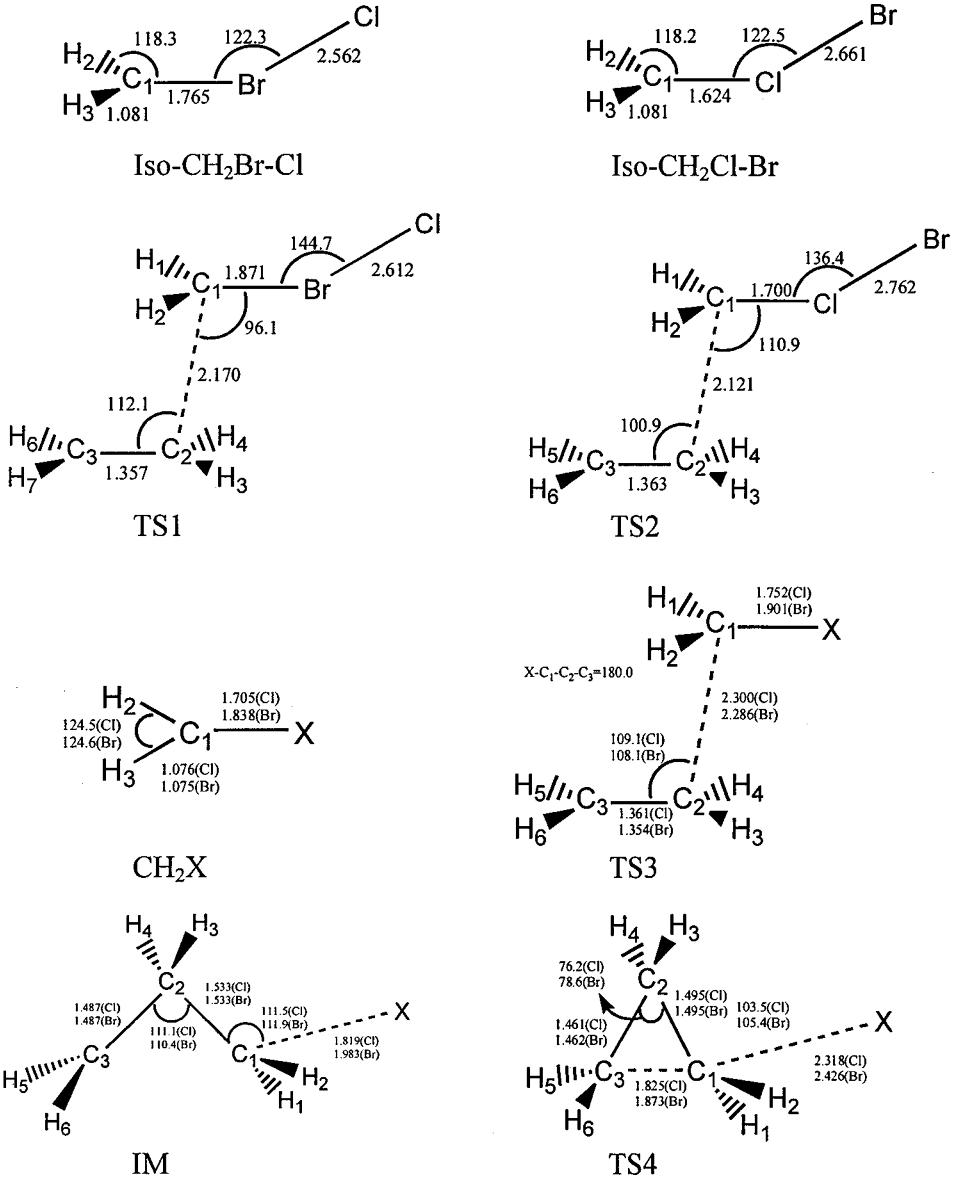

FIG. 3. Schematic diagram showing the computed optimized geometry determined from the B3LYP/6-311++G$(d,p)$ computations for the iso-CH$_2$Br-Cl, iso-CH$_2$Cl-Br, CH$_2$Br, and CH$_2$Cl species as well as the transition state(s) for the reaction of these species with ethylene to produce cyclopropane and a halogen molecule or atom leaving group [TS1=transition state for reaction of iso-CH$_2$Br–Cl with ethylene, TS2=transition state for reaction of iso-CH$_2$Cl–Br with ethylene, TS3=first transition state for reaction of CH$_2$X (X=Cl, Br) with ethylene, IM=halopropyl radical intermediate, and TS4=second transition state for reaction of CH$_2$X (X=Cl, Br) with ethylene]. Selected structural parameters are shown for each species with the bond lengths in Å and the bond angles in deg.

Reaction of iso-CH$_2$X–X with olefin

$$\text{iso-CH}_2\text{X–X}+\text{olefin}\rightarrow\text{cyclopropanated product}+\text{X}_2, \qquad (3)$$

Formation of X$_2$-olefin complex

$$\text{X}_2+\text{olefin}\Leftrightarrow\text{X}_2\text{-olefin complex}. \qquad (4)$$

We have done additional density functional theory computations to examine the reactions of iso-CH$_2$Br–Cl and iso-Cl–Br with ethylene (see Sec. II for details). The iso-CH$_2$Br–Cl and iso-CH$_2$Cl–Br systems were chosen as models for iso-polyahlomethane species containing both bromine and chlorine atoms since they are the smallest polyhalomethanes and therefore the most computationally tractable reactions to investigate. We expect that the chemical reactivity of the iso-CH$_2$Br–Cl and iso-CH$_2$Cl–Br toward ethylene (and other olefins) would be similar to the more halogenated species like iso-CHBrCl–Br and iso-CCl$_2$Cl–Br that we have experimentally observed following ultraviolet excitation of CHBr$_2$Cl and CCl$_3$Br, respectively, in the solution phase (this work). Figure 3 presents the optimized geometry determined from the B3LYP/6-311++G$(d,p)$ computations for the iso-CH$_2$Br–Cl, iso-CH$_2$Cl–Br, CH$_2$Br, and CH$_2$Cl species as well as the transition state(s) for the reaction of these species with ethylene to produce cyclopropane and a halogen molecule or atom leaving group [TS1=transition state for reaction of iso-CH$_2$Br–Cl with ethylene, TS2=transition state for reaction of iso-CH$_2$Cl–Br with ethylene, TS3=first transition state for reaction of CH$_2$X (X=Cl, Br) with ethylene, IM=halopropyl radical intermediate, and TS4=second transition state for reaction of CH$_2$X (X=Cl, Br) with ethylene]. Figure 4 shows a simple diagram depiction of the reaction pathway for the iso-CH$_2$Br–Cl, iso-CH$_2$Cl–Br with ethylene and CH$_2$Br and CH$_2$Cl with ethylene reactions with the transition state, intermediate, and product energies given relative to the separated reactants. The iso-CH$_2$Br–Cl and iso-CH$_2$Cl–Br molecules approach ethylene in an asymmetric manner attacking the CH$_2$ groups of ethylene from above the molecular plane and a transition state (TS1 or TS2) is found on the way from the reactants to

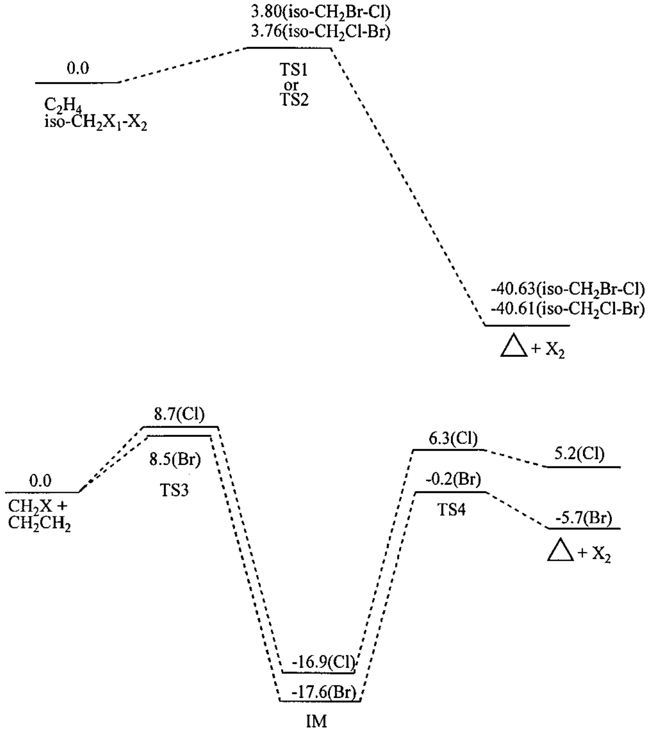

FIG. 4. Schematic diagram showing the computed relative energies (in kcal/mol) for reaction of the iso-$CH_2Br$–Cl, iso-$CH_2Cl$–Br species with ethylene and $CH_2Br$ and $CH_2Cl$ with ethylene with the transition state, intermediate, and product energies given relative to the separated reactants.

the products of cyclopropane ($C_3H_6$) and Br–Cl for each reaction. The C–C, C–Br, and Br–Cl bonds are lengthened by 0.021 Å, 0.106 Å, and 0.050 Å in the TS1 with respect to the reactant for the iso-$CH_2Br$–Cl reaction. The Cl–Br–C angle changes from 122.3° in the reactant to 144.7° in TS. The C–C, C–Cl, and Cl– Br bonds are lengthened by 0.0265 Å, 0.075 Å, and 0.100 Å in the TS2 with respect to the reactant for the iso-$CH_2Cl$–Br reaction. The Br–Cl–C angle changes from 122.5° in the reactant to 136.4° in TS. The structural changes for each reaction are consistent with the fact that intermolecular interaction is much stronger in the TS than in the reactant, which results in the intramolecular C–C and C–X bonds being weakened. IRC calculations at the UB3LYP level confirm the transition state connects the reactants of $CH_2CH_2$+iso-$CH_2Br$–Cl (or iso-$CH_2Cl$–Br) to the products of $C_3H_6$+Br–Cl.

Relative to the separated reactants, the barrier heights were calculated to be 3.80 kcal/mol and 3.76 kcal/mol for the iso-$CH_2Br$–Cl and iso-$CH_2Cl$–Br reactions with ethylene, respectively (see Fig. 4). The addition reaction between $CH_2CH_2$ and the iso-$CH_2Br$–Cl and iso-$CH_2Cl$–Br species proceeds readily via a single reaction step with a small barrier on the way to products. Results for similar calculations for the $CH_2Br$ radical and the $CH_2Cl$ radical with olefins have substantially larger barriers to reaction to give the cyclopropanated product via a two step reaction mechanism (see Fig. 4). $CH_2Br$ and $CH_2Cl$ react with ethylene and to form an intermediate Br–$CH_2CH_2CH_2$ or Cl–$CH_2CH_2CH_2$ radical which have a barrier of 17.4 kcal/mol and 23.2 kcal/mol, respectively, to go on to the cyclopropanated product ($C_3H_6$) plus halogen atom. These computational results show that the $CH_2Br$ and $CH_2Cl$ species have a difficult reaction pathway to produce a cyclopropanated product while the iso-$CH_2Br$–Cl and iso-$CH_2Cl$–Br species much more easily react with olefins to produce a cyclopropanated product (see Fig. 4). These preliminary computational results are similar to those we found previously for the iso-$CH_2Br$–Br (Ref. 52) and iso-$CH_2I$–I (Ref. 65) reactions with ethylene. These results in conjunction with experimental work[47,52,64] suggest the iso-polyhalomethane species is most likely the methylene transfer agent responsible for cyclopropanation reactions via ultraviolet photoexcitation of polyhalomethanes in the solution phase in the presence of olefins. Additional research is required to better understand the chemical reactivity of iso-polyhalomethanes in photocyclopropanation reactions of olefins. We are continuing both experimental and theoretical approaches to examine these interesting photocyclopropanation reactions for olefins and further results will be reported in due course.

### C. Possible implications for release of reactive halogens in the troposphere and stratosphere from bromine and/or chlorine containing polyhalomethanes

We have observed a number of iso-polyhalomethane species containing iodine and/or bromine atoms[47–52] as well as bromine and chlorine atoms (this work). Iso-polyhalomethanes generally have an intense electronic absorption band in the 350–500 nm region that is both greatly red-shifted and has much larger absorption coefficient than their corresponding polyhalomethane parent compound. These two characteristics of iso-polyhalomethanes suggest that they may further react photochemically in condensed phase media in the atmosphere even though they are transient species. This would be similar to the increased photodissociation rate of ozone ($O_3$) in water compared to the gas phase due to its absorption band being moderately red-shifted in water.[66] Since visible light excitation of a number of iso-polyhalomethanes in low temperature (12 K) solids leads to at least partial if not full reformation of the parent polyhalomethane molecule,[39,40] the X–X bond is likely broken to release a halogen atom following visible photoexcitation of the iso-polyahlomethane species in the condensed phase. It is not clear at this time whether or not iso-polyhalomethane species are important in the release of reactive halogens to the atmosphere, but the importance of heterogenous and/or multiphase reactions in atmospheric chemistry does suggest it would be prudent to examine the photochemical behavior of iso-polyhalomethanes.[67–94] The lifetimes (and hence the potential for photochemical release of reactive halogens) for iso-polyhalomethanes would likely increase noticeably as the temperature decreases and as the phase changes from liquid to solid.

Iso-polyhalomethane species may also act as carbenoids[52,65] and react with olefins (such as alkenes, terpenes, and other volatile organic compounds observed in the lower atmosphere)[95–105] to produce a halogen molecule product in cyclopropanation and/or other reactions. In the preceding section (Sec. III B) our preliminary quantum chemical reaction computations showed that the iso-$CH_2Br$–Cl and iso-$CH_2Cl$–Br species could react with ethylene to produce cyclopropane and Br–Cl product. This type of reaction would simultaneously release bromine and chlorine to the atmosphere. This is particularly significant since chlorine–bromine synergism[95] would result in more efficient ozone destruction from an iso-polyhalomethane species able to simultaneously release bromine and chlorine via a Br–Cl molecule. The $CHBr_2Cl$ molecule has been observed in the troposphere[92] and we have shown here that ultraviolet photolysis of $CHBr_2Cl$ in the solution phase leads to production of some iso-CHClBr–Br and iso-CHBrCl–Br. Our preliminary quantum chemical reaction calculations suggest that these iso-CHClBr–Br and iso-CHBrCl–Br species could react with olefins to release Br–Br and Br–Cl. These results suggest that the photochemistry of $CHBr_2Cl$ could have a larger impact on tropospheric ozone destruction than expected based on its gas phase photochemistry in so far as it is able to release Br–Br and Br–Cl into the troposphere via reactions of the isomer species with olefins. We note that the photochemical formation of the iso-CHBrCl–Br species from $CHBr_2Cl$ in the condensed phase and its reaction with olefins to give a Br–Cl product provides a path to release reactive chlorine into the troposphere by absorption of relatively long wavelength ultraviolet light compared to direct photochemical cleavage of a C–Cl bond by far ultraviolet light.

The photochemistry of polyhalomethanes in condensed phase environments provides two additional pathways for release of reactive halogens into the atmosphere (via photochemical and chemical reactions of the iso-polyhalomethane species) that are not available to mono-halogenmethanes like iodomethane or bromomethane. This may be important in the recent observation of iodine oxide (IO) in the marine boundary where the increase in the IO concentration was linked mainly to the change in the concentrations and photochemistry of $CH_2I_2$ and $CH_2BrI$ but not $CH_3I$.[106] The photochemical formation of isopolyhalomethanes from polyhalomethanes in condensed phase environments (such as water, ice, aerosols, etc.) provides additional pathways for depletion of the parent compound and release of reactive halogens and this could noticeably influence the atmospheric lifetimes of polyhalomethane species and estimates of their transport through the atmosphere. At this time it is not clear whether the photochemistry and chemistry of the iso-polyhalomethane species have any significant role in the chemistry of the atmosphere because there is so little known about their properties, lifetimes, photochemistry, and chemistry. A great deal of work remains to be done in order to make an assessment of their possible significance in the release of reactive halogens in the atmosphere. We are continuing our investigation of the identity, properties, lifetimes, photochemistry, and chemistry of these novel and intriguing iso-polyahlomethane species in different condensed phase environments and using a variety of experimental and theoretical techniques.

## ACKNOWLEDGMENTS

This work was supported by grants from the Research Grants Council (RGC) of Hong Kong, the Hung Hing Ying Physical Sciences Research Fund, the Committee on Research and Conference Grants (CRCG) from the University of Hong Kong, and the Large Items of Equipment Allocation 1993–94 from the University of Hong Kong.

[1] Th. Class and K. Ballschmiter, J. Atmos. Chem. **6**, 35 (1988).
[2] S. Klick and K. Abrahamsson, J. Geophys. Res., [Oceans] **97**, 12683 (1992).
[3] K. G. Heumann, Anal. Chim. Acta **283**, 230 (1993).
[4] R. M. Moore, M. Webb, R. Tokarczyk, and R. Wever, J. Geophys. Res., [Oceans] **101**, 20899 (1996).
[5] J. C. Mössigner, D. E. Shallcross, and R. A. Cox, J. Chem. Soc., Faraday Trans. **94**, 1391 (1998).
[6] C. T. McElroy, C. A. McLinden, and J. C. McConnell, Nature (London) **397**, 338 (1999).
[7] L. J. Carpenter, W. T. Sturges, S. A. Penkett, and P. S. Liss, J. Geophys. Res. [Atmos.] **104**, 1679 (1999).
[8] B. Alicke, K. Hebstreit, J. Stutz, and U. Platt, Nature (London) **397**, 572 (1999).
[9] H. E. Simmons and R. D. Smith, J. Am. Chem. Soc. **81**, 4256 (1959).
[10] D. C. Blomstrom, K. Herbig, and H. E. Simmons, J. Org. Chem. **30**, 959 (1965).
[11] N. J. Pienta and P. J. Kropp, J. Am. Chem. Soc. **100**, 655 (1978).
[12] P. J. Kropp, N. J. Pienta, J. A. Sawyer, and R. P. Polniaszek, Tetrahedron **37**, 3229 (1981).
[13] P. J. Kropp, Acc. Chem. Res. **17**, 131 (1984).
[14] M. Kawasaki, S. J. Lee, and R. Bersohn, J. Chem. Phys. **63**, 809 (1975).
[15] G. Schmitt and F. J. Comes, J. Photochem. **14**, 107 (1980).
[16] P. M. Kroger, P. C. Demou, and S. J. Riley, J. Chem. Phys. **65**, 1823 (1976).
[17] S. J. Lee and R. Bersohn, J. Phys. Chem. **86**, 728 (1982).
[18] L. J. Butler, E. J. Hintsa, and Y. T. Lee, J. Chem. Phys. **84**, 4104 (1986).
[19] L. J. Butler, E. J. Hintsa, and Y. T. Lee, J. Chem. Phys. **86**, 2051 (1987).
[20] G. Baum, P. Felder, and J. R. Huber, J. Chem. Phys. **98**, 1999 (1993).
[21] E. A. J. Wannenmacher, P. Felder, and J. R. Huber, J. Chem. Phys. **95**, 986 (1991).
[22] W. Radloff, P. Farmanara, V. Stert, E. Schreiber, and J. R. Huber, Chem. Phys. Lett. **291**, 173 (1998).
[23] S. R. Cain, R. Hoffman, and R. Grant, J. Phys. Chem. **85**, 4046 (1981).
[24] K.-W. Jung, T. S. Ahmadi, and M. A. El-Sayed, Bull. Korean Chem. Soc. **18**, 1274 (1997).
[25] S. L. Baughcum, H. Hafmann, S. R. Leone, and D. Nesbitt, Faraday Discuss. Chem. Soc. **67**, 306 (1979).
[26] S. L. Baughcum and S. R. Leone, J. Chem. Phys. **72**, 6531 (1980).
[27] J. Zhang and D. G. Imre, J. Chem. Phys. **89**, 309 (1988).
[28] J. Zhang, E. J. Heller, D. Huber, D. G. Imre, and D. Tannor, J. Chem. Phys. **89**, 3602 (1988).
[29] W. M. Kwok and D. L. Phillips, Chem. Phys. Lett. **235**, 260 (1995).
[30] W. M. Kwok and D. L. Phillips, J. Chem. Phys. **104**, 2529 (1996).
[31] W. M. Kwok and D. L. Phillips, J. Chem. Phys. **104**, 9816 (1996).
[32] S. Q. Man, W. M. Kwok, and D. L. Phillips, J. Phys. Chem. **99**, 15705 (1995).
[33] S. Q. Man, W. M. Kwok, A. E. Johnson, and D. L. Phillips, J. Chem. Phys. **105**, 5842 (1996).
[34] F. Duschek, M. Schmitt, P. Vogt, A. Materny, and W. Kiefer, J. Raman Spectrosc. **28**, 445 (1997).
[35] M. Braun, A. Materny, M. Schmitt, W. Kiefer, and V. Engel, Chem. Phys. Lett. **284**, 39 (1998).
[36] X. Zheng and D. L. Phillips, Chem. Phys. Lett. **313**, 467 (1999).
[37] J. P. Simons and P. E. R. Tatham, J. Chem. Soc. A **1966**, 854.
[38] H. Mohan, K. N. Rao, and R. M. Iyer, Radiat. Phys. Chem. **23**, 505 (1984).
[39] G. Maier and H. P. Reisenauer, Angew. Chem. Int. Ed. Engl. **25**, 819 (1986).
[40] G. Maier, H. P. Reisenauer, J. Lu, L. J. Scaad, and B. A. Hess, Jr., J. Am. Chem. Soc. **112**, 5117 (1990).
[41] L. Andrews, F. T. Prochaska, and B. S. Ault, J. Am. Chem. Soc. **101**, 9 (1979).
[42] H. Mohan and R. M. Iyer, Radiat. Eff. **39**, 97 (1978).
[43] H. Mohan and P. N. Moorthy, J. Chem. Soc., Perkin Trans. 2 **2**, 277 (1990).
[44] B. J. Schwartz, J. C. King, J. Z. Zhang, and C. B. Harris, Chem. Phys. Lett. **203**, 503 (1993).

[45] K. Saitow, Y. Naitoh, K. Tominaga, and Y. Yoshihara, Chem. Phys. Lett. **262**, 621 (1996).
[46] Å. N. Tarnovsky, J.-L. Alvarez, A. P. Yartsev, V. Sündstrom, and E. Åkesson, Chem. Phys. Lett. **312**, 121 (1999).
[47] X. Zheng and D. L. Phillips, J. Phys. Chem. A **104**, 6880 (2000).
[48] W. M. Kwok, C. Ma, A. W. Parker, D. Phillips, M. Towrie, P. Matousek, and D. L. Phillips, J. Chem. Phys. **113**, 7471 (2000).
[49] X. Zheng and D. L. Phillips, Chem. Phys. Lett. **324**, 175 (2000).
[50] X. Zheng and D. L. Phillips, J. Chem. Phys. **113**, 3194 (2000).
[51] X. Zheng, W. M. Kwok, and D. L. Phillips, J. Phys. Chem. A **104**, 10464 (2000).
[52] X. Zheng, W.-H. Fang, and D. L. Phillips, J. Chem. Phys. **113**, 10934 (2000).
[53] D. Pan, L. C. T. Shoute, and D. L. Phillips, J. Phys. Chem. A **104**, 4140 (2000).
[54] M. J. Frisch, G. W. Trucks, H. B. Schlegel *et al.*, GAUSSIAN 98, Revision A7, Gaussian, Inc., Pittsburgh, Pennsylvania 1998.
[55] A. D. Becke, J. Chem. Phys. **98**, 1372 (1993).
[56] R. Bauernschmitt and R. Ahlrichs, Chem. Phys. Lett. **256**, 454 (1996).
[57] T. H. Dunning, Jr., J. Chem. Phys. **90**, 1007 (1989).
[58] A. K. Wilson, D. E. Woon, K. A. Peterson, and T. H. Dunning, Jr., J. Chem. Phys. **110**, 7667 (2000); basis sets were obtained from the Extensible Computational Chemistry Environment Basis Set Database, Version 1.0, as developed and distributed by the Molecular Science Computing Facility, Environmental and Molecular Sciences Laboratory which is part of the Pacific Northwest Laboratory, P. O. Box 999, Richland, Washington 99352, U.S.A. and funded by the U.S. Department of Energy. The Pacific Northwest Laboratory is a multiprogram laboratory operated by Battelle Memorial Institute for the U.S. Department of Energy under Contract No. DE-AC06-76RLO 1830. Contact David Feller or Karen Schuchardt for further information.
[59] F. Bernardi, A. Bottini, J. J. W. McDougall, M. A. Robb, and H. B. Schlegel, Faraday Symp. Chem. Soc. **19**, 137 (1984).
[60] M. J. Frisch, I. N. Ragazos, M. A. Robb, and H. B. Schlegel, Chem. Phys. Lett. **189**, 524 (1992).
[61] C. Gonzalez and H. B. Schlegel, J. Chem. Phys. **90**, 2154 (1989).
[62] N. Yamamoto, T. Vreven, M. A. Robb, M. J. Frisch, and H. B. Schlegel, Chem. Phys. Lett. **250**, 373 (1996).
[63] X. Zheng and D. L. Phillips, Chem. Phys. Lett. **316**, 524 (2000).
[64] G. P. Brown and J. P. Simons, Trans. Faraday Soc. **65**, 3245 (1969).
[65] D. L. Phillips, W.-H. Fang, and X. Zheng, J. Am. Chem. Soc. (in press).
[66] M. S. Kharasch, E. V. Jensen, and W. H. Urry, J. Am. Chem. Soc. **69**, 1100 (1947).
[67] H. Taube, Trans. Faraday Soc. **53**, 656 (1957).
[68] M. J. Molina, T. L. Tso, L. T. Molina, and F. C. Y. Wang, Science **238**, 1253 (1987).
[69] M. A. Tolbert, M. J. Rossi, and D. M. Golden, Science **240**, 1018 (1988).
[70] D. Hanson and K. Mauersberger, Geophys. Res. Lett. **15**, 855 (1988).
[71] D. Hofmann, Nature (London) **337**, 447 (1989).
[72] J. Lelieveld and P. J. Crutzen, Nature (London) **343**, 227 (1990).
[73] M. J. Molina, Atmos. Environ., Part A **25A**, 2535 (1991).
[74] D. R. Hanson and A. R. Ravishankara, J. Phys. Chem. **96**, 2682 (1992).
[75] G. Brasseur and C. Granier, Science **257**, 1239 (1992).
[76] M. J. Prather, J. Geophys. Res. [Atmos.] **97**, 10187 (1992).
[77] F. J. Dentener and P. J. Crutzen, J. Geophys. Res. [Atmos.] **98**, 7149 (1993).
[78] D. R. Hanson, A. R. Ravishankara, and S. Solomon, J. Geophys. Res. [Atmos.] **99**, 3615 (1994).
[79] T. Koop and K. S. Carslaw, Science **272**, 1638 (1996).
[80] M. A. Tolbert, Science **272**, 1597 (1996).
[81] J. Reichardt, A. Ansmann, M. Serwazi, C. Weitkamp, and W. Michaelis, Geophys. Res. Lett. **23**, 1929 (1996).
[82] R. Vogt, P. J. Crutzen, and R. Sander, Nature (London) **383**, 327 (1996).
[83] D. Davis, J. Crawford, S. Liu, S. McKeen, A. Bandy, D. Thornton, F. Rowland, and D. Blake, J. Geophys. Res. [Atmos.] **101**, 2135 (1996).
[84] J. P. D. Abbatt, Geophys. Res. Lett. **24**, 1479 (1997).
[85] M. O. Andrqe and P. J. Crutzen, Science **221**, 744 (1997).
[86] B. J. Finlayson-Pitts and J. N. Pitts, Jr., Science **276**, 1045 (1997).
[87] A. R. Ravishankara, Science **276**, 1051 (1997).
[88] L. J. Liang and D. J. Jacob, J. Geophys. Res. [Atmos.] **102**, 5993 (1997).
[89] C. J. Walcek, H.-H. Yuan, and W. R. Stockwell, Atmos. Environ. **31**, 1221 (1997).
[90] K. W. Oum, M. J. Lakin, D. O. DeHaan, T. Brauers, and B. J. Finlayson-Pitts, Science **279**, 74 (1998).
[91] N. A. Clegg and R. Toumi, J. Geophys. Res. [Atmos.] **103**, 31095 (1998).
[92] L. J. Carpenter, W. T. Sturges, S. A. Penkett, P. S. Liss, B. Alicke, K. Hebestreir, and U. Platt, J. Geophys. Res. [Atmos.] **104**, 1679 (1999).
[93] B. Ramacher, J. Rudolph, and R. Koppmann, J. Geophys. Res. [Atmos.] **104**, 3633 (1999).
[94] R. Vogt, R. Sander, R. Von Glasow, and P. J. Crutzen, J. Atmos. Chem. **32**, 375 (1999).
[95] *Chemistry of Atmospheres*, 3rd ed., edited by R. P. Wayne (Oxford University Press, Oxford, 2000).
[96] H. Niki, P. D. Maker, C. M. Savage, and L. P. Breitenbach, Environ. Sci. Technol. **17**, 312A (1983).
[97] O. Horie, P. Neeb, S. Limbach, and G. K. Moorgat, Geophys. Res. Lett. **21**, 1523 (1994).
[98] S. Hatakeyama, K. Izumi, T. Fukuyama, and H. Akimoto, J. Geophys. Res. [Atmos.] **94**, 13013 (1989).
[99] P. Neeb, O. Horie, and G. K. Moortgat, Chem. Phys. Lett. **246**, 150 (1995).
[100] A. A. Chew and R. Atkinson, J. Geophys. Res. [Atmos.] **101**, 28649 (1996).
[101] N. J. Blake, D. R. Blake, T.-Y. Chen, J. E. Collins, Jr., G. W. Sachse, B. E. Anderson, and F. S. Rowland, J. Geophys. Res. [Atmos.] **102**, 28315 (1997).
[102] D. Helmig, J. Greenberg, A. Guenther, P. Zimmerman, and C. Geron, J. Geophys. Res. [Atmos.] **103**, 22397 (1998).
[103] N. M. Donohue, J. H. Kroll, J. G. Anderson, and K. L. Demerjian, Geophys. Res. Lett. **25**, 59 (1998).
[104] T. Pfeiffer, O. Forberich, and F. J. Comes, Chem. Phys. Lett. **298**, 351 (1998).
[105] S. Houweling, F. Dentener, and J. Lelieveld, J. Geophys. Res. [Atmos.] **103**, 10673 (1998).
[106] B. Alicke, K. Hebestreit, J. Stutz, and U. Platt, Nature (London) **397**, 572 (1999).